

Fabrication of porous low crystalline calcite block by carbonation of calcium hydroxide compact

Shigeki Matsuya · Xin Lin · Koh-ichi Udoh ·
Masaharu Nakagawa · Ryoji Shimogoryo ·
Yoshihiro Terada · Kunio Ishikawa

Received: 24 June 2005 / Accepted: 3 March 2006 / Published online: 3 February 2007
© Springer Science+Business Media, LLC 2007

Abstract Calcium carbonate (CaCO_3) has been widely used as a bone substitute material because of its excellent tissue response and good resorbability. In this experimental study, we propose a new method obtaining porous CaCO_3 monolith for an artificial bone substitute. In the method, calcium hydroxide compacts were exposed to carbon dioxide saturated with water vapor at room temperature. Carbonation completed within 3 days and calcite was the only product. The mechanical strength of CaCO_3 monolith increased with carbonation period and molding pressure. Development of mechanical strength proceeded through two steps; the first rapid increase by bonding with calcite layer formed at the surface of calcium hydroxide

particles and the latter increase by the full conversion of calcium hydroxide to calcite. The latter process was thought to be controlled by the diffusion of CO_2 through micropores in the surface calcite layer. Porosity of calcite blocks thus prepared had 36.8–48.1% depending on molding pressure between 1 MPa and 5 MPa. We concluded that the present method may be useful for the preparation of bone substitutes or the preparation of source material for bone substitutes since this method succeeded in fabricating a low-crystalline, and thus a highly reactive, porous calcite block.

S. Matsuya (✉)
Section of Bioengineering, Department of Dental
Engineering, Fukuoka Dental College, 2-15-1 Tamura,
Sawara-ku, Fukuoka 814-0193, Japan
e-mail: smatsuya@college.fdcnet.ac.jp

X. Lin · M. Nakagawa · R. Shimogoryo · K. Ishikawa
Department of Biomaterials, Faculty of Dental Science,
Kyushu University, 3-3-1 Maidashi, Higashi-ku, Fukuoka 812-
8582, Japan

K. Udoh
Institute of Biochemical Research and Education, School of
Medicine, Yamaguchi University, 1-1-1 Minamiogushi,
Yamaguchi 755-8505, Japan

X. Lin · Y. Terada
Department of Fixed Prosthodontics, Faculty of Dental
Science, Kyushu University, Higashi-ku, Fukuoka 812-8582,
Japan

R. Shimogoryo
Japan Institute for Advanced Dentistry, Shiba TK Building
4F, 1-8-25, Shiba, Minatoku, Tokyo 105-0014, Japan

Introduction

Calcium carbonate (CaCO_3) plays an important role in the reconstruction of bone defects as bone filler or as a source material for bone fillers. A typical example is the marine coral. Marine coral is made of aragonite-type CaCO_3 (97%<), and its skeleton with a porous microstructure is morphologically quite similar to that of human cancellous bone. The coral has been clinically used as bone substitute in dental, maxillo-facial, cranio-facial, and orthopedic surgeries for the reconstruction of bone defects [1–5]. When implanted in bone defect, it does not cause inflammatory response, shows excellent tissue response, and is gradually resorbed with time. The marine coral is also used as a source material to prepare apatite-type bone fillers. When the coral is hydrothermally treated in the presence of phosphate salts, it transforms into apatitic mineral without changing its morphology. The bone filler is called coralline apatite and has been widely used as a bone substitute in the United States [6–8].

Although the coral has some ideal characteristics as bone filler or as a source material for bone fillers, there are some drawbacks. For example, the coral suitable for bone filler can only be found in and collected from the ocean. Therefore, it costs much and is now much criticized since it destroys nature. Moreover, collected corals have to be cleaned to prevent inflammatory reaction caused by proteins and other elements present as impurities.

Drawbacks of the coral mentioned above would be solved if CaCO_3 block can be prepared artificially. One of the methods to prepare pure CaCO_3 block is the sintering of CaCO_3 powder. However, sintering process causes liberation of carbon dioxide and leads to calcium oxide formation. In addition, CaCO_3 with extremely high crystallinity is obtained even when low crystalline CaCO_3 powder is used. Unfortunately, formation of calcium oxide and high-crystalline CaCO_3 is not desirable with respect to tissue response and resorbability. On the other hand, calcium hydroxide ($\text{Ca}(\text{OH})_2$) is well known as a non-hydraulic cement in the fields of cement and concrete. When $\text{Ca}(\text{OH})_2$ is exposed to carbon dioxide that exists in air, $\text{Ca}(\text{OH})_2$ hardens and forms CaCO_3 [9–12]. However, to date, there are no reports on how to fabricate CaCO_3 block aimed for the reconstruction of bone defects based on carbonation of calcium hydroxide. In the present study, therefore, we investigated the reaction process between $\text{Ca}(\text{OH})_2$ compact and CO_2 gas, and evaluated the feasibility of CaCO_3 block preparation based on the carbonation reaction.

Materials and methods

Calcium hydroxide compact preparation

Commercially available calcium hydroxide ($\text{Ca}(\text{OH})_2$; Nacalai Tesque, Kyoto, Japan) was used in this study. The $\text{Ca}(\text{OH})_2$ powder, 0.2 g, was placed in a stainless steel mold and pressed uniaxially with an oil pressure press machine (Riken Power, Riken Seiki, Japan) under 1–5 MPa pressure. Specimens prepared were 10 mm in diameter and 1–3 mm in thickness. In a similar way, column compacts of 6 mm in diameter and 11–13 mm in height were also prepared using another stainless steel mold.

Carbonation of $\text{Ca}(\text{OH})_2$ compact

$\text{Ca}(\text{OH})_2$ compacts were placed in carbon dioxide reaction vessel for 1–72 h at room temperature for carbonation. The reaction vessel—approximately

5 L—was saturated with water vapor, and carbon dioxide gas was supplied at a rate of 0.15–0.20 L/min.

Mechanical testing

Mechanical strength of the specimens was evaluated in terms of diametral tensile strength (DTS) and compressive strength (CS) at room temperature at a constant cross-head speed of 1 mm/min on a universal testing machine (IS5000, Shimadzu, Kyoto, Japan). At least five specimens were used for each condition.

X-ray diffraction analysis

The specimens were ground into fine powders and characterized by powder X-ray diffraction (XRD) analysis. The XRD patterns of the specimens were recorded with a vertically mounted diffractometer system (RINT 2500V, Rigaku, Tokyo, Japan) using counter-monochromatized CuK_α radiation generated at 40 kV and 100 mA. The specimens were scanned from 10° to 60° 2θ in a continuous mode at a scanning rate of $2^\circ/\text{min}$. Quantitative analysis was also done on the specimens during carbonation. Calibration curve for the quantitative analysis was made using separated diffraction peaks of $\text{Ca}(\text{OH})_2$ (001, $d = 4.905 \text{ \AA}$) and calcite (0-22, $d = 2.095 \text{ \AA}$) respectively.

Microstructure

Morphology of the surfaces and fracture surfaces of the specimens was characterized by means of a scanning electron microscope (SEM; JSM 5400LV, JEOL, Tokyo, Japan) at an acceleration voltage of 15 kV after gold coating.

Porosity measurement

The apparent density of specimen was calculated from specimen's weight and dimensions. Relative density was calculated from the ratio of apparent density over the theoretical density of calcite (2.711 g/cm^3). The total porosity of specimen is then defined as

$$\text{Total porosity (\%)} = 100 (\%) - \text{Relative density (\%)}$$

Total porosity was the average value of at least five specimens.

Results and discussion

No obvious morphological changes were observed macroscopically even when the $\text{Ca}(\text{OH})_2$ compact

was exposed to carbon dioxide up to 72 h (data not shown).

Figure 1 shows the typical SEM photographs of the surfaces and fracture surfaces before and after carbonation for 1–72 h when $\text{Ca}(\text{OH})_2$ was compacted under a pressure of 1 MPa. The original $\text{Ca}(\text{OH})_2$ powder had particle size ranging from sub micron to several microns with irregular shape. As shown in Fig. 1, we found no remarkable differences before and after the carbonation process or at the time of carbonation—even at SEM level.

Figure 2 shows the typical SEM photographs of the fracture surfaces of $\text{Ca}(\text{OH})_2$ compacts prepared at various molding pressures between 1 MPa and 5 MPa after carbonation for 72 h. Basically, less pores and smaller pores were observed in the $\text{Ca}(\text{OH})_2$ compact prepared at higher pressure.

Table 1 summarizes the porosity of $\text{Ca}(\text{OH})_2$ compact when exposed to carbon dioxide for 72 h. As shown in Table 1, the porosity decreased with increase in molding pressure.

Figure 3 shows the change in powder XRD pattern of $\text{Ca}(\text{OH})_2$ compact prepared at 2 MPa for a carbonation duration of 0–72 h. As shown in Fig. 3, $\text{Ca}(\text{OH})_2$ transformed directly to CaCO_3 with time even though no morphological changes were observed with SEM. Carbonation was almost complete at 72 h. It was also shown that the CaCO_3 formed was calcite—which is the most stable phase among all CaCO_3 modifications. It has been reported that the biological properties of calcite are almost the same as those of aragonite, which is a constituent of marine coral [13]. Therefore, this calcite block is expected to show similar tissue response with marine coral if other factors, including

Fig. 1 Scanning electron microscopic observation of the surfaces and fracture surfaces of calcium hydroxide compacts under a pressure of 1 Mpa. (A and B) Before carbonation. (C and D) Carbonated for 1 h (E and F) Carbonated for 4 h (G and H) Carbonated for 72 h (A, C, E and G) Surfaces (B, D, F and H) Fracture surfaces

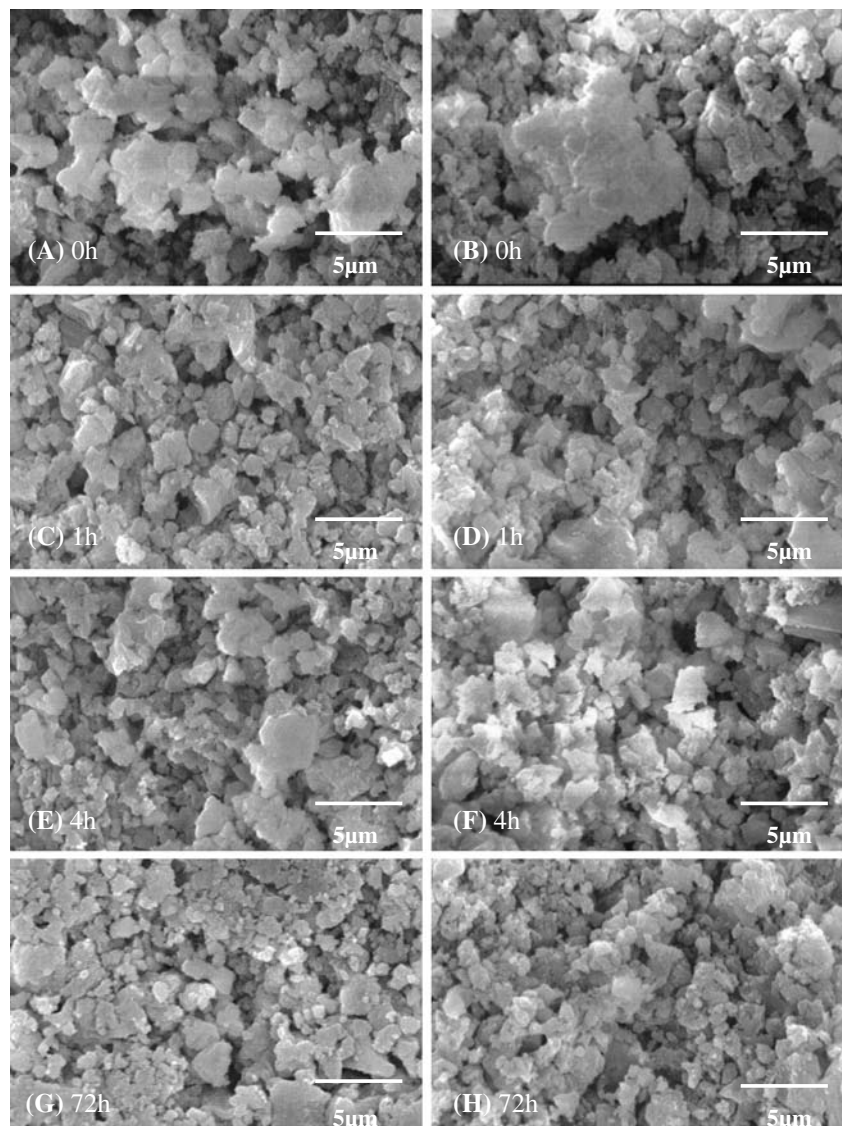


Fig. 2 Scanning electron microscopic observation of the fracture surfaces of calcium hydroxide compacts carbonated for 72 h

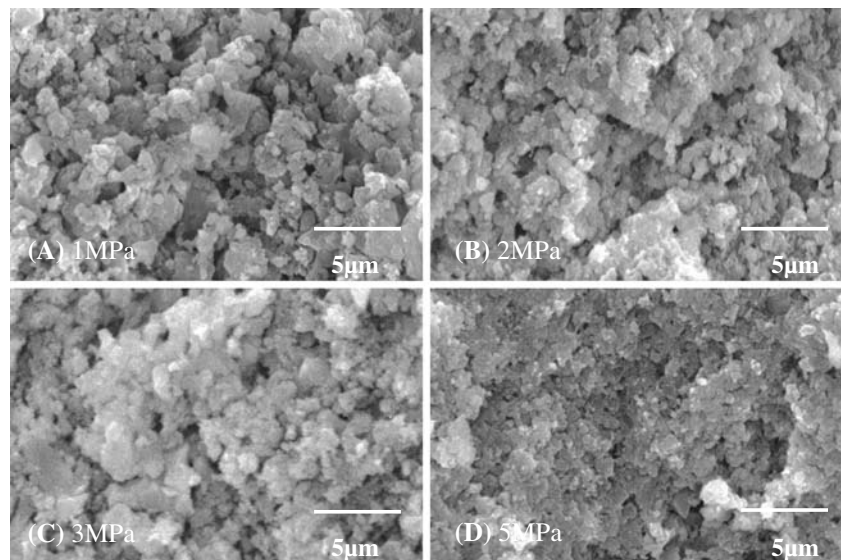


Table 1 Porosity of $\text{Ca}(\text{OH})_2$ compacts when prepared at various molding pressures and carbonated for 72 h

Molding pressure (MPa)	Porosity (%)
1	48.1 ± 1.0
2	42.2 ± 0.6
3	41.5 ± 1.6
5	36.8 ± 0.4

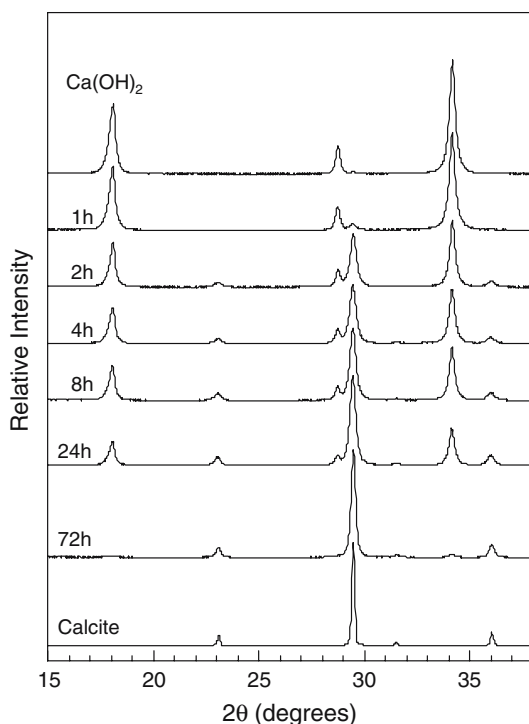


Fig. 3 Powder XRD patterns of the $\text{Ca}(\text{OH})_2$ compacts prepared at 2 MPa during carbonation for 0–72 h

morphological ones, are the same. In the XRD pattern of the specimen, peaks broader than commercially obtained CaCO_3 powder were observed, indicating that the crystallite size of calcite formed by carbonation was much smaller. Crystallite size of the specimen was estimated as 262–306 nm, whereas that of a commercial CaCO_3 powder was 834 nm. The small crystallite size may be the reason why no morphological changes were observed at SEM level even though $\text{Ca}(\text{OH})_2$ had transformed to calcite. For $\text{Ca}(\text{OH})_2$ compacts prepared at other molding pressures, the changes in XRD patterns were similar to that in Fig. 3 (data not shown).

Figure 4 shows the change with time in the amount of $\text{Ca}(\text{OH})_2$ and calcite phase in compacts subject to different molding pressures. As shown in Fig. 4, the transformation of $\text{Ca}(\text{OH})_2$ to calcite proceeded in two stages. At the first stage within 2–4 h, transformation

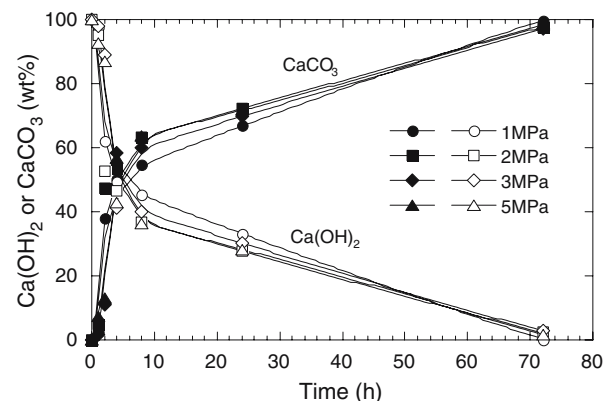


Fig. 4 Changes in the amount of $\text{Ca}(\text{OH})_2$ and calcite phase in the compacts with time at various molding pressures

was very rapid such that approximately 50% of $\text{Ca}(\text{OH})_2$ was converted to calcite. At the second stage, rate of transformation was much slower when compared to the first stage, and the remaining $\text{Ca}(\text{OH})_2$ was transformed to calcite during this stage. Basically, these tendencies were the same regardless of molding pressure. When transformation rates were compared based on molding pressure, specimens molded at lower pressure underwent faster transformation at the first stage. The second stage took a much longer time than the first stage, and thus the time required for the whole transformation was almost the same regardless of molding pressure. The two-stage transformation became much clearer when the amount of calcite formed was plotted against square root of time for a kinetic analysis, as shown in Fig. 5. At the second stage, a linear relation was observed between 2–4 h and 72 h regardless of molding pressure. The slopes, corresponding to diffusion coefficient, were almost the same regardless of molding pressure. Since a linear relation was observed at the second stage (where approximately 50% of $\text{Ca}(\text{OH})_2$ was already converted to calcite at the beginning of second stage), it could thus be suggested that carbonation rate at the second stage was controlled by diffusion process through calcite layer formed initially on the surface of $\text{Ca}(\text{OH})_2$ particles. Two candidates were proposed for the diffusion: one was CO_3^{2-} ion and the other was CO_2 gas. It was reported that the diffusion coefficient (D) of CO_3^{2-} ion for lattice diffusion in calcite was expressed by the equation, $D \text{ (cm}^2/\text{s)} = 0.65 \exp(-56,900 \text{ cal}/\text{RT})$ [14]. D at room temperature ($T = 298 \text{ K}$) is calculated as 1.2×10^{-42} , and this value led to the conclusion that the lattice diffusion of CO_3^{2-}

ion in calcite was actually negligible in the condition employed in the present study. On the other hand, carbonation of CaO at high temperature was reported to be followed by the diffusion of CO_2 gas through CaCO_3 layer formed on the surface of CaO [11, 15]. Likewise in the present $\text{Ca}(\text{OH})_2$ system, it could be thought that carbonation process at the second stage was controlled by the diffusion of CO_2 molecules through calcite layer formed initially on the surface of $\text{Ca}(\text{OH})_2$ particles.

Figure 6 shows the change of (a) DTS and (b) CS values of $\text{Ca}(\text{OH})_2$ compacts prepared at different molding pressures of 1, 2, 3, and 5 MPa as a function of carbonation time. Both DTS and CS values increased with time up to 24 h regardless of molding pressure, and they remained constant after that time period. On the other hand, higher DTS and CS values were obtained for specimens prepared under higher molding pressure. Relating these results to the data in Table 1, it was thus logical to conclude that higher mechanical strength was caused by lower porosity (Table 1).

When it comes to understanding the relationship between mechanical strength and calcite formation in

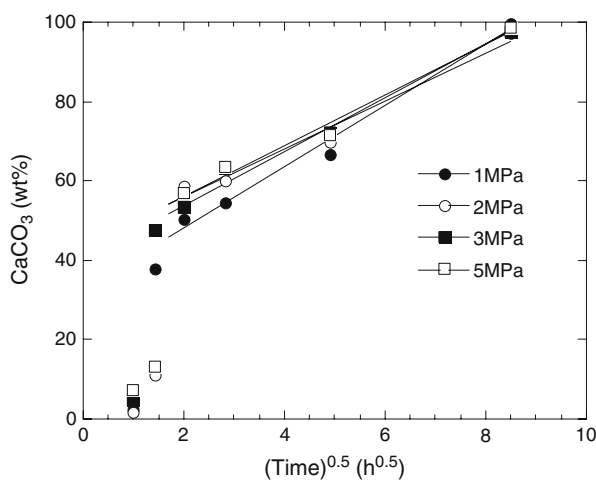


Fig. 5 Changes in the amount of calcite phase in the compacts plotted against square root of time with time at various molding pressures

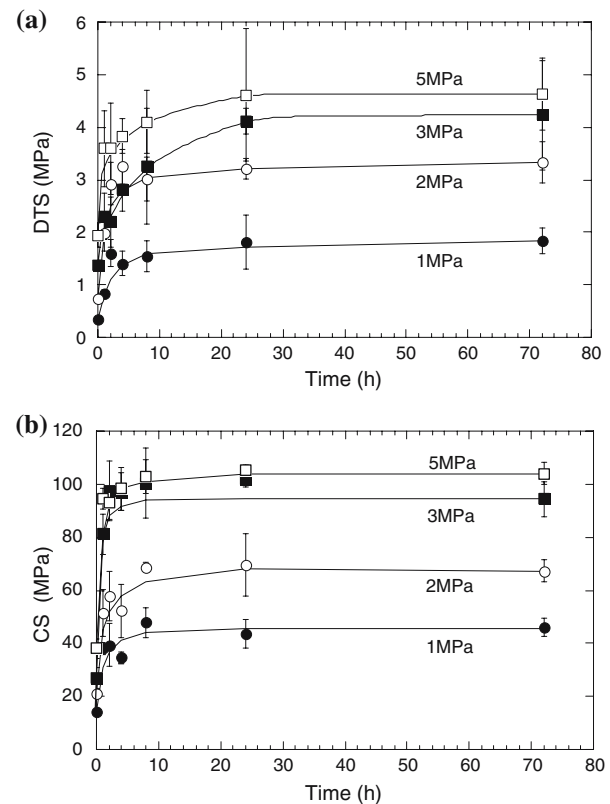


Fig. 6 (a) Changes in diametral tensile strength of compacts pressed at 1, 2, 3 and 5 MPa during carbonation with time. (b) Changes in compressive strength of column compacts pressed at 1, 2, 3 and 5 MPa during carbonation with time

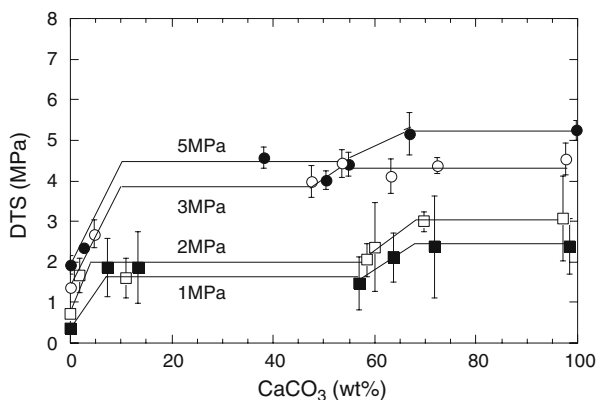


Fig. 7 Changes in DTS values of the $\text{Ca}(\text{OH})_2$ compacts prepared at various molding pressures with the amount of formed calcite

the context of the two-stage reaction process, Fig. 7 is very helpful in that the DTS values of $\text{Ca}(\text{OH})_2$ compacts prepared at various molding pressures were plotted against the amount of calcite formed. As shown in this figure, the increase of DTS could be divided into two stages. At the first stage, a rapid increase in DTS values was observed based on approximately 10%

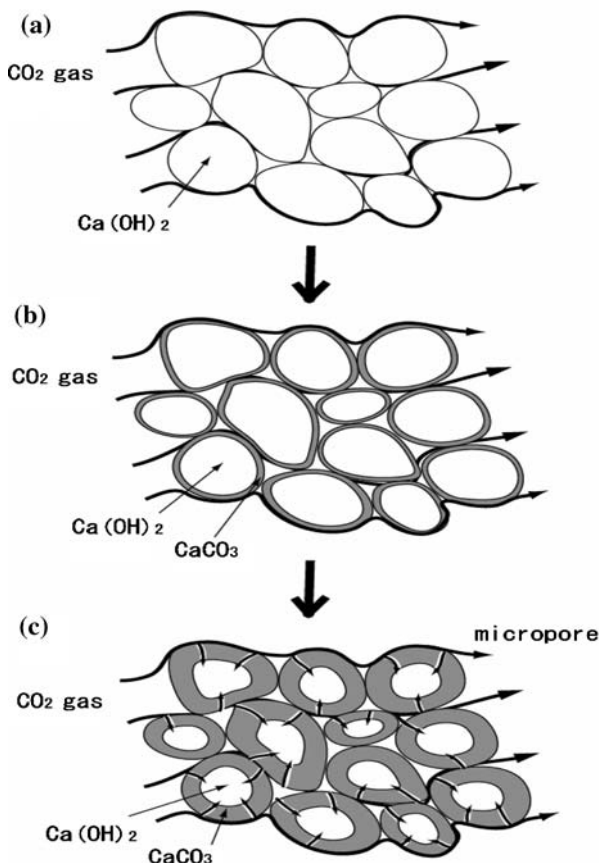


Fig. 8 The schematic model of carbonation process of $\text{Ca}(\text{OH})_2$ when exposed to CO_2 gas

calcite formation. After the initial rapid increase in mechanical strength, no increase was observed until the juncture when approximately 50% of calcite was formed. Then at the second stage, mechanical strength increased again, until approximately 50–70% of calcite was formed.

Figure 8 shows a schematic model of the carbonation process of $\text{Ca}(\text{OH})_2$. When $\text{Ca}(\text{OH})_2$ compact was exposed to CO_2 gas, the surface of $\text{Ca}(\text{OH})_2$ particles was carbonated to form a calcite layer on their surface (Fig. 8a, b). This initial process was very quick since it was only a surface reaction between $\text{Ca}(\text{OH})_2$ particles and CO_2 gas. Carbonation of the surfaces of $\text{Ca}(\text{OH})_2$ particles then resulted in an initial rapid increase in mechanical strength whereby $\text{Ca}(\text{OH})_2$ particles were bonded with the calcite crystals formed on the surface (Fig. 8b). At the second stage, further carbonation proceeded with time, although the rate of transformation was much slower than that of the initial stage. This was because carbonation reaction at this state was controlled by diffusion of CO_2 gas through micropores in calcite layer as shown in (Fig. 8c). Mechanical strength of the specimen was independent of the degree of carbonation process for a while since mechanical strength of calcium hydroxide governed the mechanical strength of the specimen at this carbonation ratio. When calcite formed was approximately 50%, mechanical strength developed further. This could be because mechanical strength of the specimen was governed by the amount of calcite formed at this stage, instead of calcium hydroxide.

Conclusions

We found that pure, low-crystalline porous calcite block with high mechanical strength could be prepared by exposing $\text{Ca}(\text{OH})_2$ compact to carbon dioxide saturated with water vapor at room temperature. Although no cell test or histological evaluation was done in the present study, low crystallinity indicates higher reactivity and resorbability. Thus calcite porous block prepared in this method is expected to be useful as a bone substitute or as a source material for the fabrication of bone substitutes.

Mechanical strength development was closely related to the transformation of $\text{Ca}(\text{OH})_2$ to calcite. Crystal morphology was the same before and after carbonation even at SEM level—which may be a good advantage for the fabrication of bone substitute blocks.

Acknowledgments This study was supported in part by a Grant-in-aid for Scientific Research from the Ministry of Education, Sports, Culture, Science, and Technology, Japan.

References

1. F. SOUYRIS, C. PELLEQUER, C. PAYROT and C. SERVERA, *J. Maxillofac. Surg.* **13**(2) (1985) 64.
2. G. GUILLEMIN, J. L. PATAT, J. FOURNIE and M. CHETAİL, *J. Biomed. Mater. Res.* **21**(5) (1987) 557.
3. J. L. PATAT and G. GUILLEMIN, *Annal. Chirur. Plast Esthet.* **34**(3) (1989) 221.
4. F. X. ROUX, D. BRASNU, B. LOTY, B. GEORGE and G. GUILLEMIN, *J. Neurosurg.* **69**(4) (1988) 510.
5. F. X. ROUX, B. LOTY, D. BRASNU and G. GUILLEMIN, *Neuro-Chirurgie* **34**(2) (1988) 110.
6. D. M. ROY and S. K. LINNEHAN, *Nature* **247** (1974) 220.
7. M. SIVAKUMAR, T. S. KUMAR, K. I. SHANTHA and K. P. RAO, *Biomaterials* **17** (1996) 1709.
8. W. SUCHANEK and M. YOSHIMURA, *J. Mater. Res.* **13** (1998) 94.
9. O. MATSUDA and H. AMADA, *Gypsum Lime* **97** (1968) 3.
10. O. MATSUDA and H. YAMADA, *Gypsum Lime* **125** (1973) 8.
11. D. R. MOOREHEAD, *Cement Concrete Res.* **16** (1986) 700.
12. O. CAZALLA, C. RODRIGUEZ-NAVARRO, E. SEBASTIAN, G. CULTRONE and M. J. TORRE DE LA, *J. Am. Ceram. Soc.* **83** (5) (2000) 1070.
13. J. C. FRICAIN, R. BAREILLE, F. ULYSSE, B. DUPUY and J. AMDEE, *J. Biomed. Mater. Res.* **42** (1998) 96.
14. D. MESS, A. F. SAROFIM and J. P. LONGWELL, *Energy Fuels* **13** (1999) 999.
15. M. CHEN, S. ITO and A. YAMAGUCHI, *J. Ceram. Soc. Jpn.* **110** (6) (2002) 512.